



Contents lists available at ScienceDirect

Biochemical Pharmacology

journal homepage: www.elsevier.com/locate/biochempharm

The synthetic bryostatin analog Merle 23 dissects distinct mechanisms of bryostatin activity in the LNCaP human prostate cancer cell line

Noemi Kedei^a, Andrea Telek^a, Alexandra Czap^a, Emanuel S. Lubart^a, Gabriella Czifra^a, Dazhi Yang^a, Jinqiu Chen^b, Tyler Morrison^b, Paul K. Goldsmith^b, Langston Lim^c, Poonam Mannan^c, Susan H. Garfield^c, Matthew B. Kraft^d, Wei Li^d, Gary E. Keck^d, Peter M. Blumberg^{a,*}

^aLaboratory of Cancer Biology and Genetics, Center for Cancer Research, National Cancer Institute, Bethesda, MD 20892, USA

^bAntibody and Protein Purification Unit, Center for Cancer Research, National Cancer Institute, Bethesda, MD 20892, USA

^cLaboratory of Experimental Carcinogenesis, Center for Cancer Research, National Cancer Institute, Bethesda, MD 20892, USA

^dDepartment of Chemistry, University of Utah, Salt Lake City, UT 84112, USA

ARTICLE INFO

Article history:

Received 19 January 2011

Accepted 22 March 2011

Available online xxx

Keywords:

Protein kinase C

Phorbol ester

Cell signaling

Bryostatin analog

ABSTRACT

Bryostatin 1 has attracted considerable attention both as a cancer chemotherapeutic agent and for its unique activity. Although it functions, like phorbol esters, as a potent protein kinase C (PKC) activator, it paradoxically antagonizes many phorbol ester responses in cells. Because of its complex structure, little is known of its structure-function relations. Merle 23 is a synthetic derivative, differing from bryostatin 1 at only four positions. However, in U-937 human leukemia cells, Merle 23 behaves like a phorbol ester and not like bryostatin 1. Here, we characterize the behavior of Merle 23 in the human prostate cancer cell line LNCaP. In this system, bryostatin 1 and phorbol ester have contrasting activities, with the phorbol ester but not bryostatin 1 blocking cell proliferation or tumor necrosis factor alpha secretion, among other responses. We show that Merle 23 displays a highly complex pattern of activity in this system. Depending on the specific biological response or mechanistic change, it was bryostatin-like, phorbol ester-like, intermediate in its behavior, or more effective than either. The pattern of response, moreover, varied depending on the conditions. We conclude that the newly emerging bryostatin derivatives such as Merle 23 provide powerful tools to dissect subsets of bryostatin mechanism and response.

Published by Elsevier Inc.

1. Introduction

Protein kinase C (PKC) has emerged as an exciting therapeutic target, reflecting its central role in cellular signaling, its differential

regulation in a range of cancers, and the identification of natural products or their derivatives targeted to PKC that have entered clinical trials [1]. The PKCs comprise a family of serine/threonine specific protein kinases, of which the classic PKC isoforms (alpha, beta1, beta2, and gamma) respond to diacylglycerol and calcium through their C1 and C2 domains, respectively, whereas the novel PKC isoforms (delta, theta, epsilon, and eta) respond only to diacylglycerol. Like most kinases, the PKCs are further regulated in a complex fashion by phosphorylation – by other serine/threonine and tyrosine specific protein kinases, by autophosphorylation, and by phosphorylation by other PKC isoforms. Diacylglycerol is a ubiquitous lipophilic second messenger, generated through the breakdown of phosphatidylinositol 4,5-bisphosphate consequent to activation of phospholipase C downstream of receptor tyrosine kinases and G-protein coupled receptors, as well as indirectly following activation of phospholipase D. Diacylglycerol recognition occurs through the C1 domains of PKC, which function as hydrophobic switches to bring about both PKC activation as well as the translocation of the PKC to membranes, enhancing its access to membrane bound substrates. Consistent with the ternary nature of the bound complex, which comprises ligand, C1 domain, and

Abbreviations: PKC, protein kinase C; DMSO, dimethylsulfoxide; ERK, extracellular signal-regulated kinases; MEK, MAPK/ERK kinase 1; MAPK, mitogen-activated protein kinase; JNK, cJun N-terminal kinases; PMA, phorbol 12-myristate 13-acetate; HAART, highly active antiretroviral therapy; DAG, diacylglycerol; GFP, green fluorescent protein; TNF-alpha, tumor necrosis factor alpha; MARCKS, myristoylated alanine rich C kinase substrate; TACE, TNF-alpha converting enzyme; TRAIL, TNF-related apoptosis-inducing ligand.

* Corresponding author at: Room 4048, Building 37, 37 Convent Drive MSC 4255, National Cancer Institute, Bethesda, MD 20892-4255, USA. Tel.: +1 301 496 3189; fax: +1 301 496 8709.

E-mail addresses: kedein@mail.nih.gov (N. Kedei), teleka@mail.nih.gov (A. Telek), alexandra.czap@gmail.com (A. Czap), lubartes@mail.nih.gov (E.S. Lubart), czifrag@gmail.com (G. Czifra), yangda@mail.nih.gov (D. Yang), chenj13@mail.nih.gov (J. Chen), morrison@gmail.com (T. Morrison), paulg@mail.nih.gov (P.K. Goldsmith), limla@mail.nih.gov (L. Lim), mannamp@mail.nih.gov (P. Mannan), garfiels@mail.nih.gov (S.H. Garfield), mkraft@chem.utah.edu (M.B. Kraft), weili@chem.utah.edu (W. Li), keck@chem.utah.edu (G.E. Keck), blumberp@dc37a.nci.nih.gov (P.M. Blumberg).

cellular membrane, emerging evidence strongly argues for the role of membrane microdomains in contributing to ligand specificity [2].

In addition to diacylglycerol, a range of complex natural products of diverse structures have been identified which function as ultrapotent analogs of diacylglycerol, binding to the C1 domain. These include the phorbol esters (diterpenes), the bryostatins (macrocyclic lactones), the indole alkaloids such as teleocidin, the polyacetates such as aplysiatoxin, and the iridals. A critical finding is that these ligands do not all induce similar biological responses upon binding. For example, whereas phorbol 12-myristate 13-acetate (PMA) is the paradigmatic mouse skin tumor promoter [3], we have shown that prostratin 13-acetate and 12-deoxyphorbol 13-phenylacetate are anti-tumor promoting [4], as is bryostatin 1 [5]. Reflecting such activities, bryostatin 1 and PEP005 (ingenol 3-angelate) are currently the subject of numerous clinical trials as anti-cancer agents (www.clinicaltrials.gov) and prostratin provides a model for overcoming resistance of cells latently infected with HIV to HAART therapy [6].

Among novel PKC ligands, the bryostatins have proven to be of particular interest [7]. Most all of the focus has been on bryostatin 1, with occasional studies examining other derivatives. Although the bryostatins function *in vitro* as activators of PKC, paradoxically in many cellular systems and for many biological endpoints they fail to induce the responses induced by the typical phorbol esters and, if administered in combination with phorbol ester, block response to the phorbol ester, showing that their failure to induce these responses is not due to instability. Mechanistic comparison reveals numerous differences that could contribute to these opposing outcomes. Bryostatin 1 shows a transient response followed by loss of responsiveness [8]. Bryostatin 1 may cause more rapid down regulation of some PKC isoforms [9,10]. Bryostatin 1 shows a unique pattern of down regulation of PKC delta, with down regulation at low concentrations but protection from down regulation at higher concentrations [11,12]. Finally, bryostatin 1 causes a distinct pattern of membrane translocation of PKC delta. Whereas PMA treatment causes initial translocation to the plasma membrane followed by subsequent distribution between plasma and internal/nuclear membranes, bryostatin 1 causes the initial translocation primarily to the internal membranes [13,14]. A critical conceptual question is whether these multiple differences in biology and in mechanism are linked to the same structural features of bryostatin 1 or whether specific structural features drive different aspects of biological response.

The small number and limited diversity of natural bryostatin derivatives, together with the daunting synthetic challenge of chemical synthesis of the bryostatins, has greatly limited understanding of bryostatin structure-activity relations. The exciting recent advances in the chemical synthesis of bryostatin and bryostatin analogs have now shattered this impasse [15]. In

their attempts to identify which features of the bryostatin 1 were dispensable for activity, thereby permitting the design of bioequivalent simplified structures with correspondingly simplified synthetic routes, the Wender group argued that the A- and B-rings of the molecule functioned as a spacer domain, whereas the active pharmacophore resided in the lower half of the molecule [16]. Experimental support for this view was provided through extensive structural comparison, showing that PKC binding activity was retained in such derivatives, and is consistent with computer modeling, indicating that it is the lower portion of the bryostatin structure which inserts into the binding cleft of the C1 domain [17].

A critical issue, however, is which structural elements confer the unique features of bryostatin 1 biological response, rather than simply PKC binding activity, since interest in the bryostatins as therapeutic agents is driven by their distinct activity as compared to the tumor promoting phorbol esters. While PKC binding activity may be necessary for activity, we found that it was not sufficient to confer a bryostatin 1-like pattern of biological response. The bryostatin derivative Merle 23, which differs from bryostatin 1 only in that it lacks four substituents in the so-called “spacer domain”, behaved in the U-937 human leukemia cell line like a phorbol ester, not like bryostatin 1 [18] (Fig. 1). Merle 23, like PMA, inhibited cell proliferation and induced attachment, whereas bryostatin 1 failed to induce either response and, in combination with Merle 23 or PMA, antagonized the response to the latter agents.

It is very important to emphasize, however, that the U-937 cell system is only one of the many systems in which the bryostatins induce a distinct pattern of biological response compared to the phorbol esters. As an initial step in developing a more robust understanding of the relationship between structural features of bryostatin analogs and their biology, we have characterized in some detail the responses of Merle 23 with those to bryostatin 1 and PMA in a second system in which bryostatin 1 acts differently from the phorbol esters. In the LNCaP human prostate cell line, phorbol esters inhibit proliferation and induce apoptosis, whereas bryostatin 1 has much less effect. Previous careful characterization of this system by others has highlighted the roles of PKC delta and tumor necrosis factor alpha in these responses, but multiple other PKC isoforms and pathways have been implicated as well [14,19–21]. We report here that, in this system, Merle 23 can be bryostatin-like, phorbol ester-like, intermediate in activity between the two, or be more active than either, depending on which specific biological or mechanistic endpoint we characterize in this system. A crucial conclusion from our findings is that the distinction between the actions of bryostatin 1 and phorbol ester is not all-or-none but rather can be dissected through structural modification. Bryostatin analogs thus should provide a powerful platform for teasing apart these response pathways and optimizing

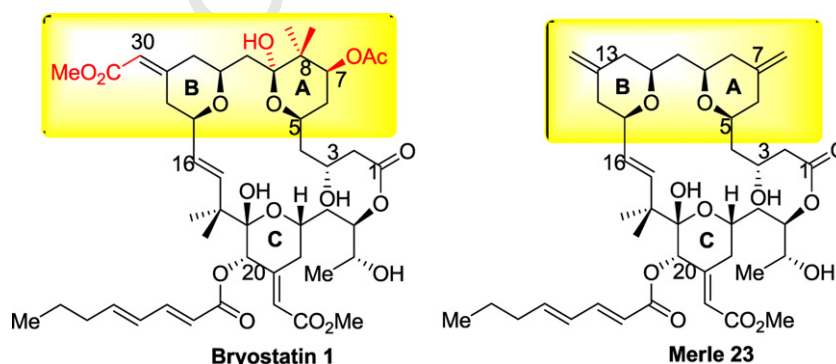


Fig. 1. Comparison of the structures of bryostatin 1 and Merle 23. The region of difference between bryostatin 1 and Merle 23 is highlighted in yellow and the specific substituents of bryostatin 1 which are lacking in Merle 23 are shown in red.

136	ligands for the desired pattern of response. Reciprocally, as better	transfection and replated onto poly-D-lysine coated 24-well plates	195
137	understanding of the interplay between the structural features of	(80,000 cells/well for proliferation and 120,000 cells/well for TNF-	196
138	bryostatin analogs and the patterns of response emerge, it should	alpha secretion).	197
139	become possible to better identify those molecular signatures of		
140	specific cancers that rationally predict that a particular bryostatin	2.4. Cell growth	198
141	analog should be therapeutically useful.		
142	2. Materials and methods		
143	2.1. Materials		
144	PMA was purchased from LC Laboratories (Woburn, MA). The	The confluency of LNCaP cells was followed in real time using an	199
145	bryostatin 1 was provided by the Developmental Therapeutics	Incucyte instrument (Essen Instruments, Ann Arbor, MI). Phase	200
146	Program, NCI (Frederick, MD). Merle 23 was synthesized as	contrast images of LNCaP cells plated onto 24-well plates (80,000	201
147	described previously [18]. The LNCaP human prostate cancer cells	cells/well) were taken every 2 h by the instrument before and after	202
148	and the K-562 human erythroleukemia cells, fetal bovine serum,	treatment for a total of 4 days. The confluency of the cells was	203
149	RPMI-1640 medium and the glutamine solution were from ATCC	calculated by the instrument's program. The proliferation of LNCaP	204
150	(Manassas, VA). Lipofectamine, Plus reagent, Lipofectamine	cells was expressed as the difference in cell confluency before and	205
151	RNAiMAX, precast 10% SDS gels, TNF-alpha Elisa kit, 7-aminoacti-	after treatment. The Incucyte permits the monitoring in parallel of	206
152	nomycin D (7-AAD), and Yo-Pro-1 were from Invitrogen (Carlsbad,	the growth and morphology in real time of cells under multiple	207
153	CA). The primary antibodies against PKC alpha (C-20), delta (C-20),	treatment conditions. K-562 cells were plated in 35 mm dishes (BD	208
154	epsilon (C-15), beta (C-16 and C-18), eta (31), theta (C-18 and 1C2),	Biosciences, Bedford, MA) at a density of 1×10^5 living cells/ml and	209
155	p65 (F-6), and cFos (H-125) were from Santa Cruz Biotechnology	24 h later were treated with different concentrations of the drugs	210
156	(Santa Cruz, CA). The primary antibodies against phosphorylated	or DMSO (diluent concentration in each sample was 0.1%). After	211
157	Y311 of PKC delta, p-ERK1/2, ERK1/2, JNK, MEK2, p-P38, P38,	72 h, the number of cells was counted using a Beckman particle	212
158	pPKD1 (Ser744), PKD1, and pMARCKS were from Cell Signaling	counter (Beckman Coulter Inc., Fullerton, CA).	213
159	(Danvers, MA), those against lamin B were from Epitomics		
160	(Burlingame, CA), those against beta-actin were from Sigma (St.	2.5. Apoptosis	214
161	Louis, MO) and those against anti-MEK1 were from Millipore		
162	(Billerica, MA). The rabbit monoclonal antibody against the p-	Apoptosis in LNCaP cells after 48 h of treatment was detected as	215
163	Ser299 of PKC delta was a custom antibody developed by Epitomics	described previously [22].	216
164	(Burlingame, CA). The horseradish peroxidase conjugated second-		
165	ary anti-rabbit antibodies, the non-fat dry milk, and the Triton X-	2.6. Measurement of TNF-alpha	217
166	100 solution were from Bio-Rad (Hercules, CA) and the ECL		
167	(electrochemiluminescence) reagent and the films were from GE	180,000 cells/well were plated into 24-well plates and treated	218
168	Healthcare (Piscataway, NJ). The FITC-conjugated goat anti-rabbit	48 h later with the indicated concentrations of the drugs. TNF-alpha	219
169	antibody and the DAPI-containing mounting medium were from	levels in the supernatants were measured with ELISA following	220
170	Vector Laboratories (Burlingame, CA). The PKC alpha (sc-44227	the manufacturer's instructions (Invitrogen, Carlsbad, CA).	221
171	and sc-36243), PKC delta (sc-44229 and sc-36253), PKC epsilon		
172	(sc-44228 and sc-36251) and control (sc-37007 and sc-44230)	2.7. Immunostaining of PKC delta	222
173	siRNAs were purchased from Santa Cruz Biotechnology (Santa		
174	Cruz, CA). Poly-D-lysine coated glass coverslips were from BD	LNCaP cells seeded onto poly-D-lysine coated coverslips 48 h	223
175	Biosciences (Bedford, MA) and the Ibi-treated dishes were from	later were treated with the indicated concentrations of PMA,	224
176	Ibidi LLC (Verona, WI). The nuclear extraction kit from Active Motif	bryostatin 1, Merle 23 or their combination for 1 h. The cells were	225
177	(Carlsbad, CA). The M-Per buffer was from Thermo Scientific	fixed with acetone, permeabilized with 0.1% Triton X-100, and	226
178	(Rockford, IL), the phosphatase and protease inhibitors, the CB1000	blocked with 1% bovine serum albumin (Sigma, St. Louis, MO) in	227
179	5-8 ampholyte premix and fluorescent pI standards used for Nano-	phosphate buffered saline (PBS) (Mediatech. Inc., Manassas, VA).	228
180	Pro technology were from Cell Biosciences (Santa Clara, CA).	After staining with anti-PKC delta primary and FITC conjugated	229
		secondary antibodies the coverslips were mounted onto micro-	230
		scope slides using DAPI-containing mounting medium and	231
		examined in a Zeiss LSM 510 confocal microscopy system (Carl	232
		Zeiss Inc, Thornwood, NY) with an Axiovert 100 M inverted	233
		microscope operating with a 25 mW argon laser tuned to 488 nm.	234
		Cells were imaged with a 63×1.4 NA Zeiss Plan-Apochromat oil	235
		immersion objective and with varying zooms (1.4–2). For more	236
		detailed description of the method see Supporting information.	237
181	2.2. Cell culture		
182	LNCaP cells and K-562 cells were cultured in RPMI-1640	2.8. Immunoblotting	238
183	containing 10% fetal bovine serum and 2 mM glutamine. For LNCaP		
184	cells experiments were performed between passage number 3 and	Immunoblotting of LNCaP cell total lysates or nuclear extracts	239
185	30. No changes in the morphology or the behavior of the LNCaP	was performed as described earlier [23]. Nuclear lysates were	240
186	cells were observed with increasing passage number. LNCaP cells	prepared using the nuclear extraction kit from Active Motif	241
187	in each experiment were manipulated 48 h after plating.	(Carlsbad, CA) following the instructions provided.	242
188	2.3. siRNA experiments		
189	Cells were plated on poly-D-lysine coated 6 cm dishes to reduce	2.9. Nano-Pro technology	243
190	the detachment of the cells after transfection with Lipofectamine		
191	RNAiMAX. Cells were transfected with a combination of equal	LNCaP cells were lysed with M-Per buffer containing phosphatase	244
192	amounts of two siRNAs at a final concentration of 60 nM.	and protease inhibitors. Lysates were mixed with CB1000 5-8	245
193	Immunoblotting was performed 48 h after transfection. For cell	ampholyte premix and fluorescent pI standards before being loaded	246
194	growth or TNF-alpha secretion cells were trypsinized 24 h after	into the NanoPro1000 system (Cell Biosciences, Santa Clara, CA) for	247
		analysis. Nano-Pro is an automated capillary based iso-electric	248

249 focusing (IEF) immunoassay system developed by Cell Biosciences
250 (Santa Clara, CA). Iso-electric focusing was performed in capillaries
251 filled with a mixture of cell lysate (in this study, approximately
252 10–20 ng protein), fluorescently labeled pI standards, and ampho-
253 lytes and locked into place by using UV light followed by
254 immunoprobings with anti-Erk1/2, anti-MEK1, anti-MEK2 or anti-
255 JNK antibodies. The signal was visualized by ECL and was captured
256 by a CCD camera. The digital image is analyzed and quantified with
257 Compass software (Cell Biosciences, Santa Clara, CA). For more
258 detailed information see the Supporting information.

259 2.10. Translocation of GFP-tagged PKC isoforms in LNCaP cells

260 Translocation of PKC isoforms in LNCaP cells plated on ibi-treated
261 dishes was evaluated as described before [23]. Supporting
262 information contains a more detailed description of the experiment.

263 2.11. Statistical analysis

264 Statistical significance was determined using the Student's
265 two-tailed *t*-test.

266 3. Results

267 3.1. Depending on conditions, Merle 23 can resemble either bryostatin 268 1 or PMA in its effects on growth, apoptosis, and TNF-alpha secretion of 269 LNCaP cells

270 We have previously described that Merle 23 behaves like PMA
271 and not like bryostatin 1 in inhibiting the growth of U-937
272 leukemia cells and inducing their attachment [18]. To extend our
273 comparison of the actions of bryostatin 1 and Merle 23, we have
274 now examined the behavior of Merle 23 in the human
275 erythroleukemia cell line K-562 and the LNCaP human prostate
276 cell line. In the K-562 cells used previously for testing bryostatin 1
277 like compounds [24], it is established that PMA inhibits, while
278 bryostatin 1 has only limited effects on cell growth [25]. In LNCaP
279 cells that are well characterized for the biological responses
280 induced by different PKC ligands, PMA inhibits cell growth and
281 induces TNF-alpha secretion and apoptosis, whereas bryostatin 1
282 fails to do so [14,20]. In K-562 cells, similarly to U-937 cells, Merle
283 23 was PMA-like for inhibiting cell growth in a dose dependent
284 manner (Fig. 1A).

285 In contrast to the results in the U-937 and K-562 leukemia cells,
286 in the LNCaP cells Merle 23 resembled bryostatin 1 and not PMA,
287 neither inhibiting cell growth (Fig. 2B) nor inducing apoptosis (Fig.
288 2C). Cell cycle analysis gave similar results (Supplementary Figure
289 1C). In addition, although Merle 23 caused a measurable increase
290 in TNF-alpha secretion compared to bryostatin 1 ($p = 0.006$), this
291 effect was very much less than that for PMA (Fig. 2D). Like
292 bryostatin 1, the action of Merle 23 was dominant over that of
293 PMA, indicating that the lack of effect was not because of instability
294 of Merle 23 under the assay conditions. The combination of Merle
295 23 with PMA prevented the inhibition of cell growth (Supplemen-
296 tary Figure 1A) and the induction of apoptosis (Supplementary
297 Figure 1B) by PMA.

298 On the other hand, the pattern of behavior of Merle 23 relative
299 to bryostatin 1 and PMA depended very much on the specific
300 conditions. Motivated by our mechanistic analysis, described
301 further below, showing differences among the compounds in the
302 rates of PKC isoform down regulation, we examined the effect of
303 two well characterized proteasome inhibitors, lactacystin and MG-
304 132, on the pattern of response. We found that both proteasome
305 inhibitors shifted the response of the LNCaP cells to Merle 23 from
306 bryostatin-like to PMA-like. In the presence of the proteasome
307 inhibitors at concentrations that did not have any effect on vehicle

308 treated control cells, Merle 23 caused comparable inhibition of cell
309 growth as did PMA (Fig. 2E). Bryostatin 1 was also affected but to a
310 much more modest degree. TNF-alpha secretion by PMA was
311 increased by the proteasome inhibitors and the effects of Merle 23
312 and PMA became similar, whereas the level of TNF-alpha induced
313 by bryostatin 1 remained very low (Fig. 2F). Multiple mechanisms
314 must contribute to the induction of TNF-alpha secretion in
315 response to PMA, as evidenced by the biphasic nature of the dose
316 response curve (Fig. 2D). Lactacystin eliminated most of the
317 biphasic pattern of induction by PMA or Merle 23, while there was
318 still a suggestion of biphasic induction for bryostatin 1 (Supple-
319 mentary Figure 1D).

320 These findings afford two clear conclusions. First, the pattern of
321 response to Merle 23 relative to bryostatin 1 and PMA is not
322 uniform for a single biological endpoint but depends on the cell
323 type. In the U-937 and K-562 human leukemia cells Merle 23 is
324 PMA-like, inhibiting cell growth (Fig. 2A and [18]), but in the LNCaP
325 cells Merle 23 is bryostatin-like, failing to inhibit cell growth.
326 Second, the pattern of response of Merle 23 within a single cell type
327 can be modulated by other agents. In the LNCaP cells, Merle 23
328 shifted from bryostatin-like to PMA-like in the presence of a
329 proteasome inhibitor.

330 3.2. Role of individual PKC isoforms in biological response to Merle 23 331 in the LNCaP cells

332 Among PKC isoforms, PKC alpha, delta and epsilon are the
333 predominant isoforms expressed in LNCaP cells, whereas PKC beta,
334 eta, and theta are undetectable [14,20] (and data not shown). PKC
335 delta has been suggested to be the major isoform in the LNCaP cells
336 responsible for the inhibition of cell growth and for TNF-alpha
337 secretion upon PMA treatment [21,26], although a role for PKC
338 alpha [19,27] and for PKC epsilon in the inhibition of growth has
339 also been suggested [28]. To verify the isoform(s) responsible for
340 the different biological effects of the compounds under our specific
341 assay conditions, we first examined the effect of PKC inhibitors.
342 Gö6976 is known to inhibit the activity of classical PKC isoforms
343 (PKC alpha in LNCaP cells) and of PKDs [29]; Gö6983 inhibits the
344 activity of all PKC isoforms but not that of PKD1 [30]. The general
345 PKC inhibitor Gö6983 but not Gö6976 blocked the inhibition of cell
346 growth by PMA (Fig. 3A). These results argue that the activity of
347 one or more of the novel PKC isoforms (PKC delta or epsilon) is
348 critical in the inhibition of growth by PMA and suggest a defect in
349 the activation of the relevant novel PKC(s) by Merle 23 and
350 bryostatin 1.

351 As a second approach to define the role of specific PKC isoforms,
352 we examined the effect of isoform knockdown by siRNA treatment.
353 To achieve effective knockdown without undue toxicity and
354 detachment of cells, we needed to modify the plating conditions of
355 the LNCaP cells to use poly-D-lysine coated plates. Under these
356 conditions, we were able to efficiently suppress expression of PKC
357 alpha, delta, and epsilon individually (Supplementary Figure 2). As
358 described above, we had observed that the bryostatin-like or the
359 PMA-like behavior of Merle 23 was subject to modulation. For the
360 LNCaP cells on the poly-D-lysine coated plates, we found that Merle
361 23 was intermediate between PMA and bryostatin 1, causing a
362 partial suppression of growth (compare controls without siRNA,
363 Fig. 3B). This response was thus somewhat different from what we
364 observed on the cells plated under standard conditions. Knock-
365 down of PKC delta by siRNA largely (65%) prevented the growth
366 inhibition induced by PMA and prevented the partial inhibition
367 observed for Merle 23 (Fig. 3B). Treatment with scrambled siRNA
368 or siRNA against PKC alpha or epsilon had no effect.

369 The PKC isoform dependence of TNF-alpha secretion was
370 similar to that for cell growth but not identical. Here, Gö6976, the
371 inhibitor of the classic PKC isoforms, caused a 47% reduction in

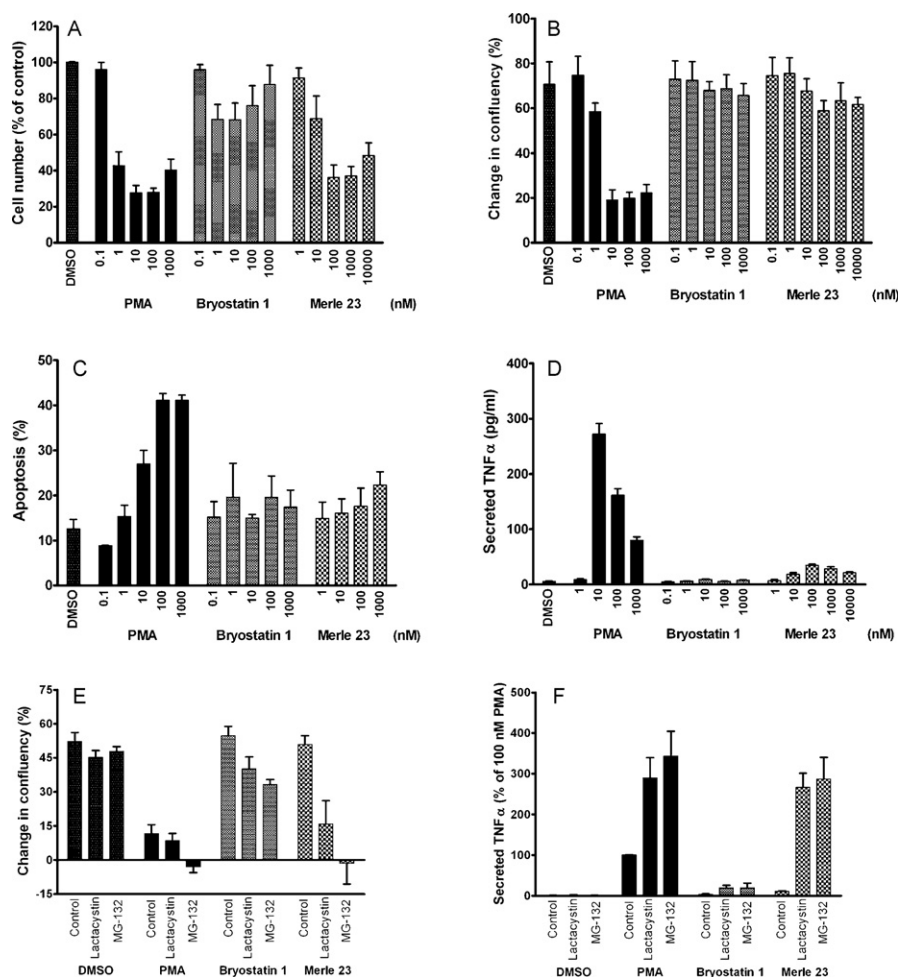


Fig. 2. Biological responses induced by PMA, bryostatin 1 and Merle 23 in K-562 and LNCaP cells. (A) The effect of PMA, bryostatin 1, and Merle 23 on K-562 cell growth. 72 h after treatment with DMSO as control or of the indicated concentrations of the different drugs the number of cells was counted by a particle counter. Values represent the mean \pm S.E.M. of three independent experiments. Merle 23 1000 nM versus PMA 1000 nM, $p = 0.71$; versus bryostatin 1 1000 nM, $p = 0.013$. (B) The effect of PMA, bryostatin 1, and Merle 23 on cell growth represented by the difference in confluency of the cells before treatment and 72 h later. Confluency was calculated by the Incucyte instrument from phase contrast images taken every 2 h during the experiment. Values represent the mean \pm S.E.M. of four independent experiments. Merle 23 1000 nM versus PMA 1000 nM, $p = 0.0036$; versus bryostatin 1 1000 nM, $p = 0.82$. (C) Apoptosis induced by PMA, bryostatin 1, and Merle 23 was detected by FACS analysis of 7-AAD and Yo-Pro stained cells after 48 h treatment. Values represent the mean \pm S.E.M. of three independent experiments. Merle 23 1000 nM versus PMA 1000 nM, $p = 0.0038$; versus bryostatin 1 1000 nM, $p = 0.37$. (D) TNF- α secreted into the supernatant of LNCaP cells treated for 24 h with PMA, bryostatin 1, and Merle 23 was measured by ELISA. Values represent the mean \pm S.E.M. of three independent experiments. 1000 nM PMA versus 10 nM PMA, $p = 0.0007$. (E) The effect of proteasome inhibitors lactacystin (2 μ M) and MG-132 (1 μ M) on cell growth in the presence of vehicle (DMSO) or 100 nM PMA, bryostatin 1 or Merle 23 was determined by Incucyte as described for (A). Values represent the mean \pm S.E.M. of five independent experiments. Merle 23 + Lactacystin and Merle 23 + MG-132 versus PMA + Lactacystin and PMA + MG-132, $p = 0.52$ and 0.88 , respectively; bryostatin 1 versus PMA, both in the presence of MG-132, $p < 0.0009$. (F) The effect of proteasome inhibitors lactacystin (2 μ M) and MG-132 (1 μ M) on TNF- α secretion induced by 24-h treatment with 100 nM PMA, bryostatin 1 or Merle 23. Values represent the mean \pm S.E.M. of four independent experiments. PMA versus PMA + MG-132, $p = 0.0016$; PMA + MG-132 versus Merle 23 + MG-132, $p = 0.53$; bryostatin 1 versus PMA, both in the presence of MG-132, $p = 0.0065$.

response to PMA (Fig. 3C). Likewise, a similar reduction was observed upon suppression of PKC alpha by siRNA (Fig. 3D). For comparison, suppression of PKC delta caused a 77% reduction in PMA-induced TNF-alpha secretion. We conclude that, under our experimental conditions, PKC delta is the predominant PKC isoform mediating the responses to PMA for growth and for TNF-alpha secretion but that PKC alpha also makes a contribution to the latter response. The most straightforward prediction is that the failure or reduced effectiveness of Merle 23 or bryostatin 1 to induce these responses reflects defects in their abilities to activate or maintain in an activated state PKC delta (and PKC alpha), at least within a specific target region.

3.3. Changes in the signaling downstream of PKC in response to Merle 23, PMA and bryostatin 1

To better compare the effects of Merle 23 with bryostatin 1 and PMA we characterized the time and dose dependence of their

actions on proximate targets in PKC signaling pathways and on PKC isoforms (next section). We quantitatively determined the activation of MAPK pathways (MEK/ERK and JNK phosphorylation) using Nano-Pro technology and we detected phosphorylation of the known PKC substrates MARCKS and PKD1 by immunoblotting. The Nano-Pro technology separates the individual phosphorylation states of a protein and allows quantitative comparison of their levels [31]. We detected these changes early, at 30 min after treatment, at 60 min, when the penetration of the compounds is more complete, and at 150 min, to evaluate the duration of signal activation. Merle 23 showed a pattern similar to that of PMA and bryostatin 1 at 30 min for increasing the level of P-ERK1, PP-ERK1 and P-ERK2 (Fig. 4A), as well as for phosphorylation of JNK, MEK1 and MEK2 (Supplementary Figure 3 A–C) but was somewhat less potent (e.g. 1.7-, 3.5-, and 3.1-fold less potent relative to bryostatin 1 for P-ERK1, PP-ERK1, and P-ERK2, respectively, fold differences calculated from EC₅₀ values). At 150 min, phosphorylation of ERK1/2 and JNK in response to bryostatin 1 had returned to the basal

388
389
390
391
392
393
394
395
396
397
398
399
400
401
402
403
404
405

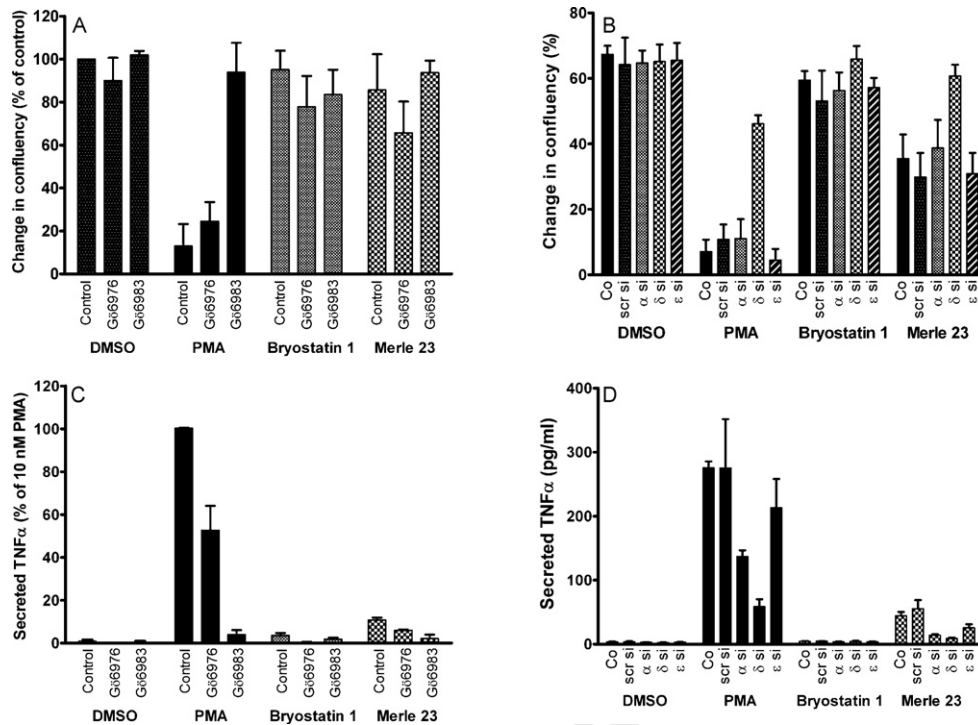


Fig. 3. Evaluation of the role of individual PKC isoforms in the biological effects of PMA, bryostatin 1 and Merle 23 using PKC inhibitors or siRNA. (A) The effect of PKC inhibitors Gö6976 (2 μ M) and Gö6983 (2 μ M) on cell growth in the presence of vehicle (DMSO) or 100 nM PMA, bryostatin 1 or Merle 23 was determined by the Incucyte as described for Fig. 2A. Values represent the mean \pm S.E.M. of three independent experiments. PMA versus PMA + Gö6983, $p = 0.0091$; PMA versus PMA + Gö6976, $p = 0.44$. (B) The effect of different siRNAs on cell growth. Cells were transfected with the indicated siRNAs as described in Section 2 and were treated 48 h later with DMSO as control or 300 nM PMA, bryostatin 1 or Merle 23 for 48–60 h. Confluency was determined by the Incucyte. Values represent the mean \pm S.E.M. of seven independent experiments. Co = control, non-treated cells; scr = scrambled siRNA; α , δ , ϵ si = siRNA against PKC alpha, delta and epsilon isoforms, respectively. p values for Merle 23 control versus DMSO, PMA and bryostatin1 control are 0.0015, 0.0046 and 0.010, respectively; p values for delta siRNA versus control for PMA and Merle 23 are $p < 0.0001$ and 0.014; all p values for PMA and Merle 23 between control and alpha or epsilon siRNAs are >0.5 . (C) The effect of PKC inhibitors Gö6976 (2 μ M) and Gö6983 (2 μ M) on TNF-alpha secretion induced by 10 nM PMA, bryostatin 1 or Merle 23. Secretion of TNF-alpha into the supernatants was measured by ELISA 24 h after treatment. Values represent the mean \pm S.E.M. of three independent experiments. PMA versus PMA + Gö6976, $p = 0.0005$. (D) The effect of different siRNAs on TNF-alpha secretion. Cells transfected with the indicated siRNAs as described in Section 2 were treated 48 h later with DMSO as control or 10 nM PMA, 100 nM bryostatin 1 or 100 nM Merle 23 for 24 h. TNF-alpha secreted into the supernatant was measured by ELISA. Values represent the mean \pm S.E.M. of three independent experiments. For abbreviations see legend above. PMA versus PMA + alpha siRNA, $p = 0.0006$.

level. In contrast, response to PMA and to Merle 23 was more sustained, indicating that Merle 23 was more PMA-like than bryostatin-like for these endpoints in the LNCaP cells. Similar changes in ERK1/2 phosphorylation at 30, 60 and 150 min were detected by conventional immunoblotting (Fig. 4B–4D) (We also tried to measure phosphorylation of p38 MAPK but were unable to get a reliable signal). In addition to the change in the extent of phosphorylation with time, it was also evident that the potency of Merle 23 and PMA was shifted to the left at 150 min compared to 30 min (about 7.8-fold increase in potency for Merle 23 and about 9.9-fold for PMA (bryostatin 1 could not be evaluated because of the lack of response at 150 min) (Fig. 4A), suggesting that at 30 min the effect of Merle 23 or PMA had not reached a steady state, whether due to slow penetration or whether due to lack of balance between phosphorylation and dephosphorylation.

Merle 23 also induced similar levels of phosphorylation at 30 min of two well known PKC substrates, MARCKS and PKD1, as did PMA and bryostatin 1, but Merle 23 was less potent, at least for PKD1 phosphorylation (Fig. 4B). The 60 min (Fig. 4C) and 150 min (Fig. 4D) incubation times revealed that for these responses, as for MEK/ERK and for JNK phosphorylation, the effect of bryostatin 1 was the most transient; that of Merle 23 and PMA was less so.

At 60 min another PKC activation dependent signal, expression of the immediate early gene product cFos [32], became detectable. As with the other signaling responses, Merle 23 was somewhat less potent than PMA and bryostatin 1 for inducing cFos expression and was intermediate in its duration of response (Fig. 4C and D, Supplementary Figure 4A and 4B). The PMA-induced signal was

sustained, detectable up to 8 h (Supplementary Figure 4B), and the response induced by bryostatin 1 had already decreased at 150 min and was almost undetectable at 6 h (Supplementary Figure 4A). We conclude that, for a number of these downstream responses in LNCaP cells, Merle 23 showed a duration of response intermediate between those of bryostatin 1 and PMA. Its duration tended, however, to be closer to that of PMA than to that of bryostatin 1 and it clearly could not be characterized as bryostatin 1-like. Previously, sustained activation or ERK [20] and/or JNK signaling [33,34] were proposed as underlying mechanisms for the apoptotic effect of phorbol esters in LNCaP cells.

3.4. The effect of Merle 23 on the phosphorylation, down-regulation and subcellular localization of different PKC isoforms

Next, we evaluated the effects of Merle 23 on the phosphorylation, down-regulation, and translocation of PKC isoforms and compared these responses with those to PMA and to bryostatin 1, with particular focus on PKC delta. For PKC delta, phosphorylation at Ser299 has been described as reflecting the activated state of the enzyme [35]. Phosphorylation of PKC delta at Tyr 311 has been shown to alter its activity and behavior [36–38], although its specific role in most responses remains unclear. We find that at all time points Merle 23 was appreciably less potent than either PMA and bryostatin 1 for activation of PKC delta, as reflected by phosphorylation at Ser299, while the PMA and bryostatin 1 responses were almost indistinguishable (30 min, Fig. 4B; 60 min, Fig. 4C; 150 min, Fig. 4D; 6 h, Supplementary Figure 4A). For

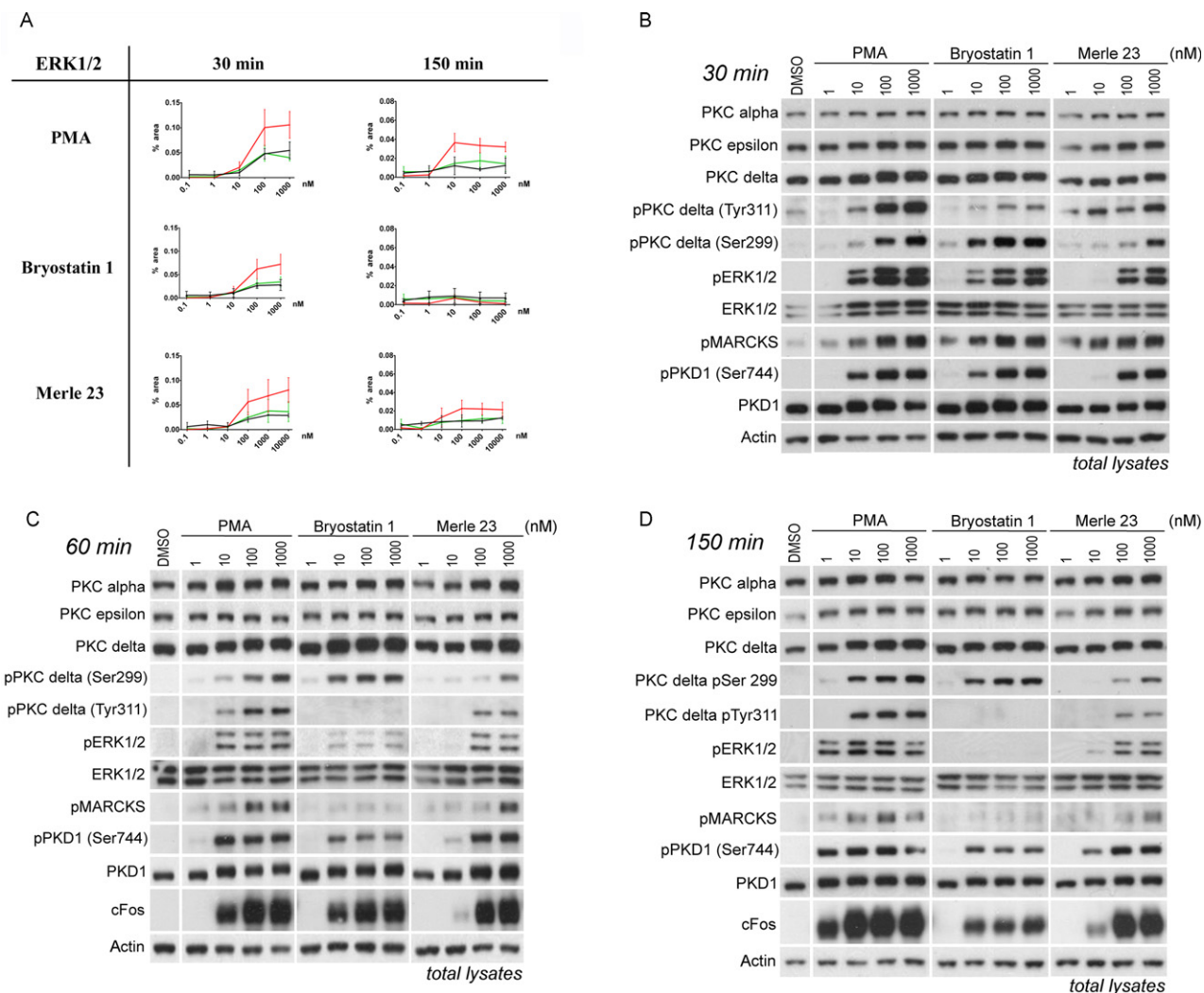


Fig. 4. Activation of PKC-responsive signaling pathways in LNCaP cells after treatment with PMA, bryostatatin 1 or Merle 23. (A) ERK1/2 activation was quantitatively measured using Nano-Pro technology as described in Section 2 in total cell lysates treated for 30 and 150 min with the indicated concentrations of PMA (0.1–1000 nM), bryostatatin 1 (0.1–1000 nM) or Merle 23 (0.1–10000 nM). Red line: pp-ERK1, black line: pp-ERK2; green line: p-ERK1. Data represent the mean \pm S.E.M. of three independently performed experiments. At 150 min the ppERK1 signal induced by Merle 23 was significantly different from that of bryostatatin 1 ($p = 0.012$). (B–D) Changes in signaling detected by immunoblotting in total cell lysates from cells treated for 30 min (B), 60 min (C) or 150 min (D) with the indicated concentrations (1–1000 nM) of PMA, bryostatatin 1, or Merle 23. Actin levels were evaluated as controls for equal protein loading. Data in (B)–(D) are representative of three independent experiments.

inducing tyrosine phosphorylation at Y311, all three compounds showed large differences from one another. PMA induced a strong and sustained phosphorylation, Merle 23 induced a weaker and more transient phosphorylation, while the phosphorylation induced by bryostatatin 1 was very weak and transient, detectable only at 30 min (Fig. 4B–D, Supplementary Figure 4A). Merle 23 becomes even more PMA-like when the more extensive down-regulation of PKC delta is taken into account by normalizing the Tyr 311 phosphorylation results to total PKC delta levels (Supplementary Figure 4C, see below for discussion of down-regulation of PKC delta). Of particular note, the central role for PKC delta in the action of PMA for inhibiting cell growth and inducing TNF-alpha secretion, as evidenced both from the literature and from our own studies described above, lead to the strong prediction that bryostatatin 1 and Merle 23 should be defective in PKC delta activation, at least for some cellular subcompartment. The results for S299 phosphorylation argue that this is not the case, at least at earlier times, for total PKC delta, and for sufficient concentrations of the two ligands.

Down-regulation subsequent to ligand binding is a potential feedback mechanism for PKC, curtailing activation of PKC signaling pathways [39–42]. It also provides one surrogate

measure for ligand interaction in cases for which reagents for direct detection of PKC isoform activation are not available. In the LNCaP cells, down-regulation in response to phorbol ester treatment is typically observed between 4 and 24 h [20]. We find that Merle 23, bryostatatin 1, and PMA show clearly distinct patterns of down-regulation of the PKC isoforms, as measured in whole cell lysates. Merle 23 was unique in being the most efficient for down-regulating PKC delta (detectable already at 6 h), but the least efficient for down-regulating PKC alpha. It was PMA-like for down-regulating PKC epsilon and PKD1 (Fig. 5 and Supplementary Figure 4A). Bryostatatin 1, on the other hand, induced biphasic down-regulation of PKC delta, as has been described for it previously in multiple cell lines [11,12]. It was the most potent and efficient in down-regulating PKC alpha, and it was the least potent in down-regulating PKC epsilon and PKD1. PMA seemed to be equally potent for down-regulation of all PKC isoforms and of PKD1. The different patterns of down-regulation of PKC isoforms by Merle 23 as compared to bryostatatin 1 and PMA argues that Merle 23 cannot be simply regarded as lying somewhere on a continuum of activity between bryostatatin 1 and PMA. Rather, Merle 23 is a unique compound with a unique spectrum of effects on down-regulation.

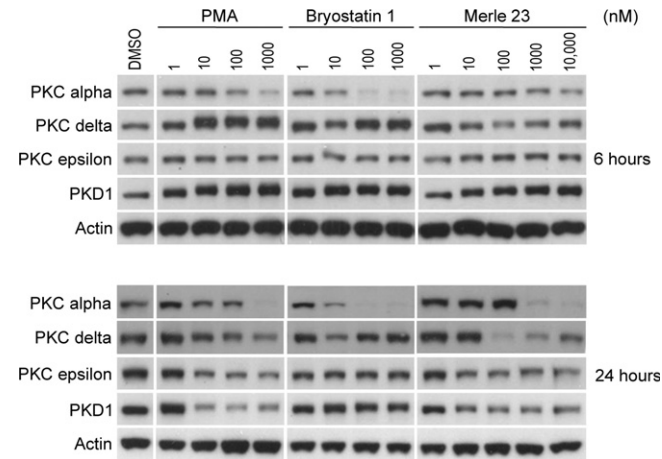


Fig. 5. Down-regulation of different PKC isoforms in LNCaP cells after 6- and 24-h treatment. The levels of the indicated PKC isoforms and of actin as loading control were detected by immunoblotting in total cell lysates from cells treated for 6 or 24 h with the indicated concentrations (1–1000 nM) of PMA, bryostatin 1 or Merle 23. The data are representative of at least three independent experiments.

Translocation of PKCs from cytoplasm to different membrane structures including plasma membrane, nuclear membrane, and mitochondria is another hallmark of their activation [13,14,19,40]. It is of functional importance, since the subcellular localization of PKCs determines the available substrates, the partner proteins

with which they can form complexes, their posttranslational modifications and their fate (such as tyrosine phosphorylation or ubiquitination followed by degradation). In addition to examining PKC isoform levels and phosphorylation in total cell lysates as a function of time and dose of Merle 23, bryostatin 1, or PMA, as described above, we also looked at a nuclear enriched membrane subfraction, prepared under conditions optimized for evaluating nuclear translocation of transcription factors (Active Motif, Carlsbad, CA). This fractionation revealed further differences between ligands beyond those observed in the total lysates.

Merle 23 induced a pattern different from that of either PMA or bryostatin 1 for the translocation of PKCs to the nuclear enriched subcellular fraction (Fig. 6A and B, compare with Fig. 4C and Supplementary Figure 4A for total lysates). Merle 23, similarly to PMA, induced translocation of PKC alpha and epsilon in a dose dependent manner, albeit with lower potency than PMA, while bryostatin 1 induced only a partial translocation at 60 min. On the other hand Merle 23, like bryostatin 1, failed to efficiently translocate PKC delta and PKD1 (Fig. 6A). (Note that part of the total PKC delta is already in this subcellular fraction without any treatment unlike PKC alpha, epsilon or PKD1) (Fig. 6A, B, D). At 6 h the differences were even more pronounced. For PKC alpha and epsilon Merle 23 is PMA-like but for PKC delta and PKD1, especially pPKD1, Merle 23 is more bryostatin 1-like (Fig. 6B).

The amount of PKCs present in any of the subcellular fractions, including nuclear enriched fractions, depends not only on the efficiency of translocation but also on the amount of total protein,

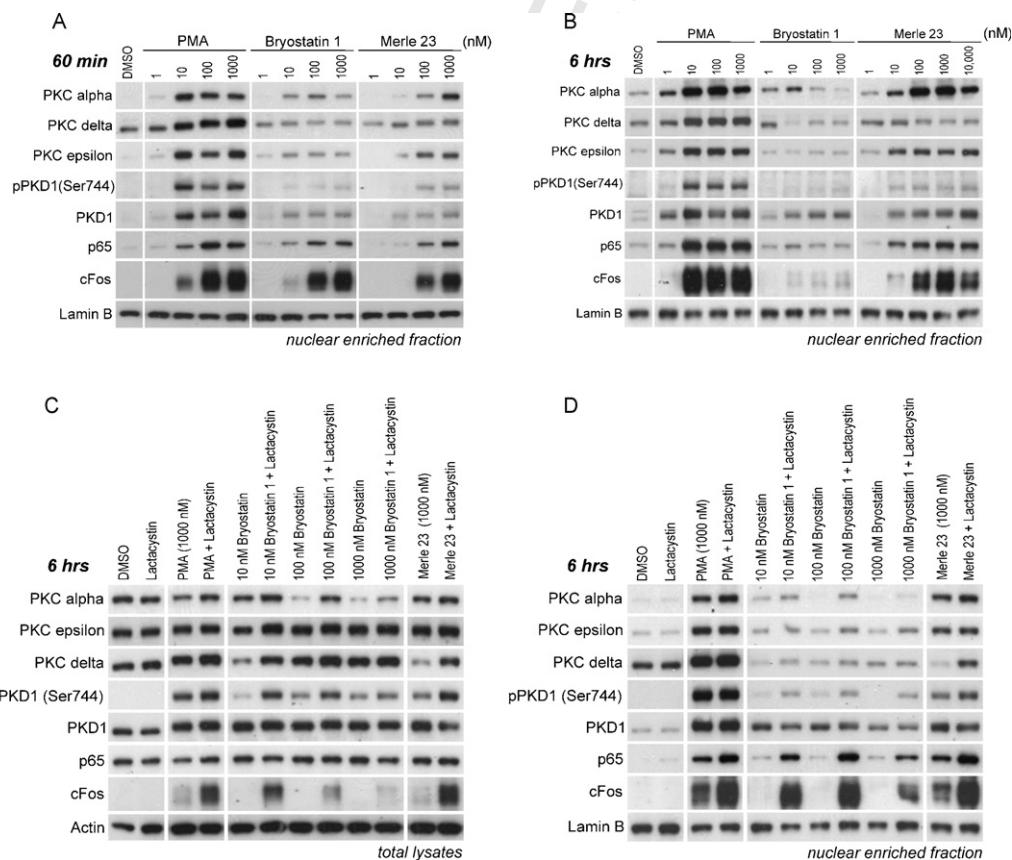


Fig. 6. Analysis of different PKC isoforms in the nuclear-enriched fraction from LNCaP cells after treatment with PMA, bryostatin 1 or Merle 23. (A) Detection of different PKC isoforms in the nuclear-enriched subcellular fraction of LNCaP cells treated for 60 min with the indicated concentrations of PMA, bryostatin 1 or Merle 23. Lamin B levels were evaluated as controls for equal protein loading. The levels of proteins in the total cell lysates are presented in Fig 4C. (B) Detection of different PKC isoforms in the nuclear-enriched subcellular fraction of LNCaP cells treated for 6 h with the indicated concentrations of PMA, bryostatin 1 or Merle 23. Lamin B levels were evaluated as controls for equal protein loading. The levels of proteins in the total cell lysates are presented in Supplementary Figure 4A. (C and D) The levels of the PKC isoforms or other proteins were determined by immunoblotting in the total lysates (C) or nuclear enriched fractions (D) of LNCaP cells treated with the indicated concentrations of PMA, bryostatin 1, Merle 23 alone or in combination with 2 μ M lactacystin for 6 h. Results are representative of three independent experiments.

536 especially at later time points (6 h) when some of the isoforms such
537 as PKC alpha and PKC delta may be significantly down-regulated.
538 When the proteasome inhibitor lactacystin was co-administered
539 with Merle 23, down-regulation of PKC delta was prevented and
540 the amount of PKC delta in the total cell lysates (Fig. 6C) and
541 nuclear extracts (Fig. 6D) was increased. In contrast, treatment
542 with lactacystin had little effect on nuclear PKC delta in the
543 presence of bryostatin 1 and PMA. As shown in Fig. 2D and E,
544 cotreatment with the proteasome inhibitors lactacystin and MG-
545 132 converted the more bryostatin-like effects of Merle 23 to more
546 PMA-like for cell growth and TNF-alpha secretion, with much
547 lesser effects on bryostatin 1. These results focus attention on the
548 PKC delta present in the nuclear-enriched fraction as contributing
549 to induction of these biological responses. It should be emphasized,
550 however, that proteasome inhibitors have many effects. Lactacystin
551 partially prevented the bryostatin 1 induced down-regulation
552 of PKC alpha and increased the level of PKC alpha present in the
553 nuclear-enriched fraction at 6 h (Fig. 6C and D). In addition, the
554 proteasome inhibitors will necessarily affect many cellular
555 processes in addition to down-regulation of PKCs [43].

556 The nuclear enriched fractionation protocol was one optimized
557 to evaluate translocation of transcription factors to the nucleus.
558 We therefore examined translocation of p65 and cFos, members of
559 the NFκB and AP1 family of transcription factors respectively,
560 which are prominently involved in PKC signaling [44]. Merle 23,
561 PMA, and bryostatin 1 induced similar translocation of p65 and
562 cFos to the nuclear enriched fraction (Fig. 6A). The duration of the
563 response to Merle 23 was similar to that for PMA, while the effect
564 of bryostatin 1 was very transient as indicated by the low p65 and
565 cFos levels in this fraction at 6 h (Fig. 6B).

566 Although lacking in resolution, translocation of exogenously
567 expressed, GFP-labeled PKC isoforms provides a real time
568 measure of their response to ligands. GFP-PKC alpha and GFP-
569 PKC epsilon translocate to the plasma membrane; GFP-PKC delta,
570 on the other hand, shows a complex pattern of translocation to the
571 plasma membrane and internal membranes both as a function of
572 time and of the ligand, for which hydrophobicity is one critical
573 determinant [13,14]. Of particular relevance, we had reported that
574 in Chinese hamster ovary cells PMA caused initial translocation of
575 GFP-PKC delta to the plasma membrane, with subsequent
576 equilibration to internal membranes, especially the nuclear
577 membrane but not inside the nucleus, whereas bryostatin 1
578 already at early times caused the translocation to internal
579 membranes [13].

580 In the present study with the LNCaP cells, we have also used
581 immunostaining of endogenous PKC delta (Fig. 7A) as well as
582 overexpression of exogenous GFP-PKC delta (Fig. 7B). We find the
583 expected difference between PMA and bryostatin 1 for the pattern of
584 translocation of PKC delta with both methods. PKC delta localized mainly to
585 the plasma membrane after PMA treatment, while it localized
586 mostly to cytoplasm and to internal membranes, including nuclear
587 membrane, after treatment with bryostatin 1. As for many
588 biological responses (inhibition of cell growth and apoptosis
589 (Supplementary Figure 1A and 1B)) the effect of bryostatin 1 for
590 translocation was dominant over that of PMA (Fig. 7A). Merle 23
591 was different from both PMA and bryostatin 1 for the pattern of
592 endogenous PKC delta localization as it showed staining in the
593 cytoplasm and some in the plasma membrane (Fig. 7A). For the
594 translocation of overexpressed GFP-PKC delta, Merle 23 induced
595 translocation mostly to internal membranes, resembling bryostatin
596 1 (Fig. 7B). The results obtained with the two different methods
597 thus gave somewhat different results for Merle 23, presumably
598 reflecting the influences of fixation or of the expression level of PKC
599 delta. Nonetheless, overall the findings for localization again
600 suggest that Merle 23 is intermediate between PMA and bryostatin
601 1 in its behavior.

4. Discussion

602 Taming of the bryostatin chemistry has been a pressing
603 objective. First, bryostatin 1 is a natural product, available only
604 in vanishingly small quantities upon isolation from *Bugula meritina*
605 [7]. The limited availability of bryostatin 1 has thus impacted both
606 clinical trials and mechanistic analysis. A practical synthesis could
607 alleviate this issue of supply. Second, synthesis of simplified
608 structural derivatives could identify which parts of the complex
609 structure of bryostatin 1 are essential for activity and which are
610 dispensable, potentially identifying bioequivalent analogs that
611 could be made more readily. While this objective in the first
612 instance has been directed at simplified derivatives based on the
613 bryostatin structure as a template, the extension of this objective
614 could be to adapt those essential structural features to other high
615 affinity PKC ligand templates such as the DAG-lactones, which are
616 synthetically much more accessible.

617 These intense synthetic efforts are now yielding structures for
618 probing of bryostatin structure activity relations, albeit for the
619 most part as yet in very limited quantities. Initial analysis has used
620 either binding to PKC or inhibition of leukemia cell growth,
621 typically of the K-562 leukemia cells [16,17]. The conclusion from
622 these studies was that the A- and B-rings of bryostatin 1 were
623 simply a "spacer domain", restricting the conformation of the
624 lower portion of the molecule so that it bound with high affinity to
625 the binding cleft of the C1 domain of PKC, but was otherwise
626 uninvolved.

627 In marked contrast to this concept of the A- and B-rings as a
628 spacer domain, we reported that Merle 23, which only differs from
629 bryostatin 1 in its less extensive functionalization on these two
630 rings, acted like a phorbol ester in the U-937 human leukemia cells
631 and failed to show the unique pattern of biological activity of
632 bryostatin 1 [18]. In this system, further structure activity analysis
633 has shown that Merle 27, which restores the C-7 acetate
634 substituent missing from Merle 23, still behaved like PMA [45],
635 whereas both Merle 28, lacking the C30 carbomethoxy group from
636 the B-ring of bryostatin 1 [46] and Merle 30, lacking the C9-
637 hydroxyl group from the A-ring [47] displayed bryostatin-like
638 biology in these cells. In initial studies, this latter compound was
639 also bryostatin-like for proliferation and TNF-alpha secretion in the
640 LNCaP cells, although it was not characterized in further detail
641 [47]. All the compounds were potent for binding to PKC.

642 These studies unambiguously demonstrated a critical role for
643 the A- and B-ring substituents of the bryostatin 1 in conferring the
644 unique pattern of biological response, at least for the two
645 endpoints examined and for the U-937 cells. Here, we confirmed
646 that Merle 23 behaves in the K-562 leukemia cell line like it does in
647 the U-937 cells. A separate issue was the generality of this
648 conclusion over a broader range of cellular responses as well as
649 over aspects of the signaling pathways directly coupled to
650 bryostatin 1 action, namely regulation of PKC isoforms and those
651 downstream responses closely linked to their activity.

652 The initial system we chose to address this broader issue was
653 that of the LNCaP human prostate cancer cells. Multiple groups
654 have shown that PMA and bryostatin behave differently in this
655 system, with PMA inhibiting cell growth and inducing apoptosis
656 whereas bryostatin is much less effective for doing so. Such
657 studies, moreover, have already characterized in some detail
658 relevant signaling pathways involved in these responses to
659 phorbol ester and started to define the role of individual PKC
660 isoforms. These responses include sustained activation of the p38,
661 JNK MAPK cascade [33,34,48], sustained membrane-translocation
662 of PKC alpha resulting in sustained activation of the ERK MAPK
663 cascade [20], and inhibition of the AKT pathway [48]. PKC delta
664 mediated RhoA, ROCK activation leading to transcriptional
665 activation of p21^{CIP1} [49], and membrane localized, activated
666

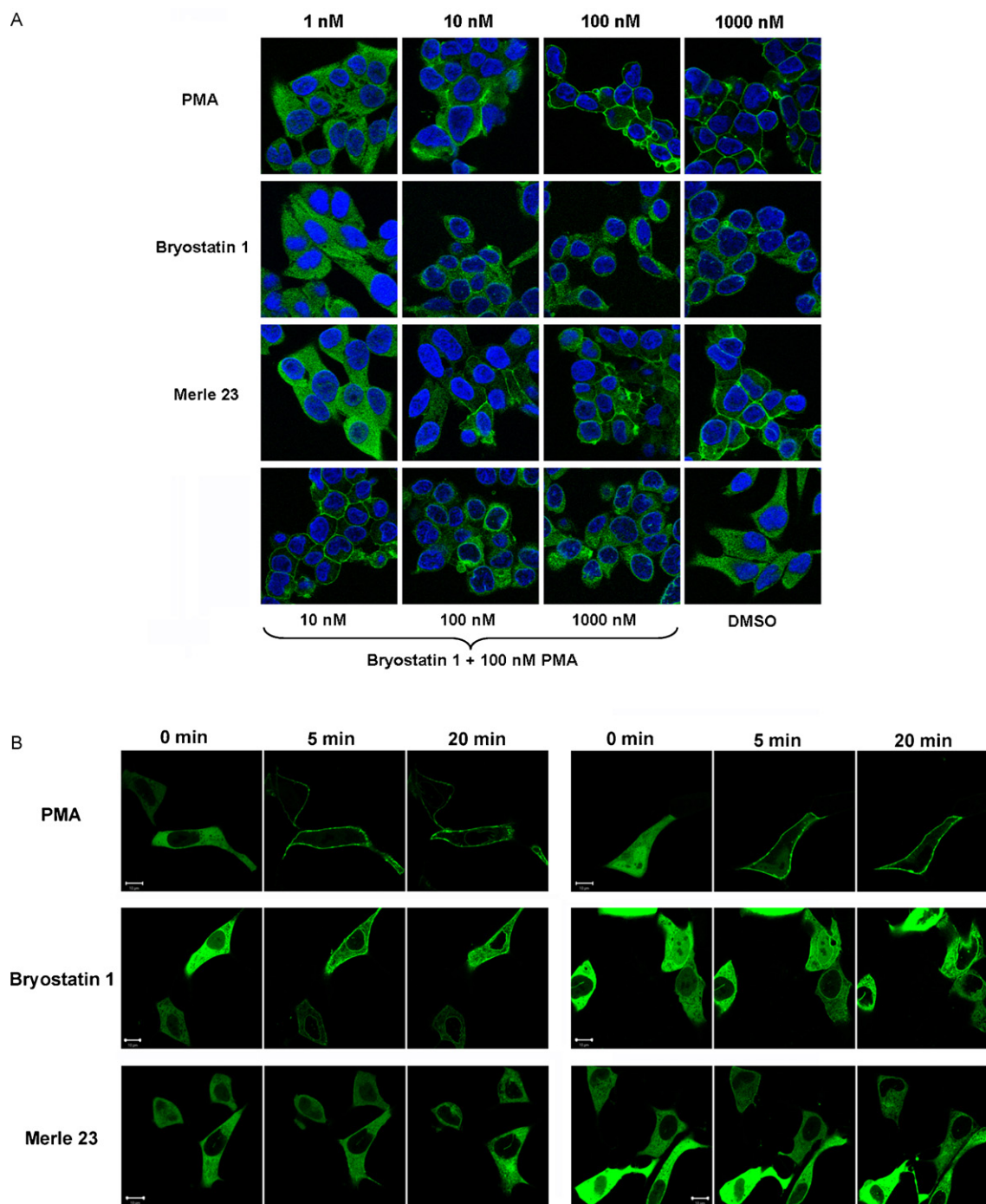


Fig. 7. Localization of PKC delta in LNCaP cells following treatment with PMA, bryostatin 1 or Merle 23. (A) Subcellular localization of endogenous PKC delta in LNCaP cells 60 min after treatment with the indicated concentrations of PMA, bryostatin 1, Merle 23 or the combination of 100 nM PMA and 10, 100, 1000 nM bryostatin 1. The immunostaining was performed as described in Section 2. (B) Translocation of GFP-PKC delta in LNCaP cells. LNCaP cells plated on ibidi treated dishes for better attachment were transfected to express GFP-PKC delta and 24 h later were treated with 1000 nM PMA, bryostatin 1 or Merle 23. The translocation of GFP-PKC delta was detected by confocal microscopy in real time with images taken every 30 s. Images of two representative cells taken at 0, 5 and 20 min are shown. The data presented in each panel are representative of four independently performed experiments.

667 PKC delta caused activation of TACE, release of the death factors
 668 TRAIL and TNF alpha, and downstream activation of the extrinsic
 669 apoptotic cascade and activation of JNK, p38 MAPK and caspases
 670 [21,50]. Additionally, phorbol ester was reported to cause
 671 activation of the intrinsic apoptotic pathway by phosphorylation
 672 of BAD independently of Akt, ERK or p90Rsk [51]; it induced
 673 downregulation of ATM resulting in activation of ceramide
 674 synthase and ceramide release [52]; and led to nuclear accumula-
 675 tion of phosphorylated p53 [53]. The involvement of PKC isoforms

in these responses is complex. PKC alpha and delta are described as
 contributing to the apoptosis induced by phorbol ester [19–21],
 whereas PKC alpha was thought to play the major role for another
 class of PKC ligands, the DAG-lactones [27]. In the case of
 bryostatin 1, the overexpression (individually) of either PKC alpha
 [20] or PKC epsilon [28] has been reported to change its behavior to
 now act like PMA. While the responses of the LNCaP cells to PKC
 activation must thus be highly complex, suggesting that differ-
 ences in ligand action may be found at multiple levels, the LNCaP

676
 677
 678
 679
 680
 681
 682
 683
 684

Table 1
Summary of the biological responses induced by PMA, bryostatin1 and Merle 23 in LNCaP cells.

	PMA			Bryostatin 1			Merle 23		
Biological responses									
Inhibition of growth			+			–			– or +/-*
Apoptosis			+			–			– or +/-*
Secretion of TNF-alpha			+			–			+/-
+ Lactacystin			++			–			++
Signaling pathways									
ERK1/2, JNK			+/sustained			+/transient			+/intermediate
AP1 and NFkB activation (nuclear cFos and p65)			+/sustained			+/transient			+/intermediate
Activities on PKCs	PMA			Bryostatin 1			Merle 23		
	α	δ	ε	α	δ	ε	α	δ	ε
Phosphorylation of PKC delta at 1 h									
Ser 299		+			+			+	
Tyr 311		+			–			+ +/-	
Down-regulation of different PKCs									
6 h	+/-	–	–	++	+/-†	–	–	+	–
24 h	+	+	+	++	+†	–	+	++†	+
Subcellular localization									
Endogenous PKCs in the nuclear enriched fraction									
30 min	+	+	+	+/-	–	+/-	+	+/-	+/-
6 h	+	+	+	+/-	–	–	+	–	+
Endogenous PKC delta		Plasma membrane			Internal membranes			Plasma and internal membranes	
Translocation of GFP-PKC delta		Plasma membrane			Mostly internal membranes			Mostly internal membranes	

* When cells plated onto poly-D-lysine coated plates.

† Biphasic.

system promised the opportunity, at the very least, to obtain rich comparative signatures of the actions of Merle 23, PMA, and bryostatin 1. It should be emphasized, however, that the pattern of response of the LNCaP cells is not representative of more aggressive prostate cancer cells. It is well established that prostate cancer cell lines such as PC-3 or DU145 do not show growth inhibition in response to PMA [22,54]. Our goal rather was to use the LNCaP system to develop insights into the behavior of Merle 23.

Our findings provide a very clear conclusion regarding Merle 23. Depending on the response, Merle 23 can be bryostatin-like, PMA-like, intermediate in its behavior, or have greater effect than either. Our findings show that the four missing substituents on the A- and B-rings, which distinguish Merle 23 from bryostatin 1, are not required for all of the differential responses to bryostatin 1. On the other hand, for the majority of endpoints examined (Table 1), Merle 23 indeed much more resembled PMA than it did bryostatin 1. Furthermore, the behavior of Merle 23 is dependent on the cellular context, as illustrated by the effect of the proteasome inhibitors or of different plating conditions. We conclude that there is not a single pharmacophore conferring a bryostatin-like as distinct from a phorbol ester-like pattern of response.

The diversity of patterns of response at the biological level is entirely consistent with the diversity of the pattern of effects of Merle 23, PMA, and bryostatin 1 on their proximal targets, the PKC isoforms. As shown previously in LNCaP cells and in many other cellular systems, bryostatin 1 was very efficient in down-regulating PKC alpha [9,10,40] and it induced a biphasic down-regulation of PKC delta [11,12] with almost no effect on PKC epsilon and PKD1. Merle 23 was uniquely potent for down-regulating PKC delta, was the least potent for down-regulating PKC alpha and was very similar to PMA for PKC epsilon and PKD1. Likewise, the three compounds had distinct effects for translocation of different PKC isoforms, as measured by subcellular fractionation. Merle 23, like PMA and unlike bryostatin 1, induced translocation of PKC alpha and PKC epsilon to the nuclear enriched subcellular fraction. On the other hand, like bryostatin 1 and unlike PMA, Merle 23 failed to induce translocation of PKC delta to the same compartment. While our nuclear enriched subcellular fraction may include contributions from other membrane frac-

tions, the critical observation is that the patterns of distribution driven by the three ligands are distinct. Finally, the three compounds had distinct actions on the patterns of regulatory phosphorylation of PKC delta. All caused phosphorylation at Ser299, a regulatory site which reflects enzyme activation. On the other hand, bryostatin 1 was virtually unable to induce tyrosine phosphorylation at Y311, whereas Merle 23 was almost as effective as PMA. Phosphorylation at this site is thought to influence both stability and specificity [36–38]. Our studies highlight the appreciation that ligands for C1 domains cannot be understood simply at the level of binding affinity for some PKC isoforms. Their relative affinities at PKC isoforms with potentially opposite biological effects, such as PKC delta and epsilon, their differential localization to membrane compartments or subcompartments, and the complex feedback among their targets can all contribute to very different outcomes.

While our goal in the LNCaP cells was to conduct a broad-based comparison of Merle 23 with PMA and bryostatin 1, rather than to resolve the complex mechanisms underlying the regulation of growth and apoptosis by such agents in the LNCaP cells, our data are largely consistent with the suggestion of Kazanietz, using somewhat different experimental conditions [14], that failure to properly localize activated PKC delta is an important contributor to the pattern of response for TNF-alpha secretion and inhibition of proliferation in this system. Thus, levels of PKC delta in the nuclear enriched fraction mirrored the responses to PMA, bryostatin 1, and Merle 23 both in the presence and absence of the proteasome inhibitors. In the case of Merle 23, down-regulation of PKC delta may make a larger contribution to the loss of PKC delta in this compartment; in the case of bryostatin 1, failure of the existing PKC delta to localize may be more important. Our analysis provided less support for the suggestion that plasma membrane localization of PKC delta was critical, at least under our conditions.

At this very early stage of exploration of the structure activity relations of bryostatin analogs, the richness of opportunity for identification of novel spectra of response is already apparent. Myalgia is the limiting toxicity that has emerged for bryostatin 1, whereas it has not been described for other PKC targeted drugs [55]. The diversity of patterns of response provides encouragement

that designed analogs of bryostatin can be developed possessing a specific spectrum of the desired bryostatin attributes. Additionally, as we develop more detailed insights into the effects of such derivatives on signaling pathways, it may be possible to better match specific derivatives with those specific cancers in which these pathways are relevant.

Acknowledgements

This research was supported in part by the Intramural Research Program, National Institutes of Health, Center for Cancer Research, National Cancer Institute and by Grant GM28961 to GEK.

Appendix A. Supplementary data

Supplementary data associated with this article can be found, in the online version, at doi:10.1016/j.bcp.2011.03.018.

References

[1] Kazanietz MG. Protein kinase C in cancer signaling and therapy. New York/Dordrecht/Heidelberg/London: Springer; 2010.

[2] Duan D, Sigano DM, Kelley JA, Lai CC, Lewin NE, Kedei N, et al. Conformationally constrained analogues of diacylglycerol. 29. Cells sort diacylglycerol-lactone chemical zip codes to produce diverse and selective biological activities. *J Med Chem* 2008;51:5198–220.

[3] Hecker E. Cocarcinogenic principles from the seed oil of *Croton tiglium* and from other Euphorbiaceae. *Cancer Res* 1968;28:2338–49.

[4] Szallasi Z, Krsmanovic L, Blumberg PM. Nonpromoting 12-deoxyphorbol 13-esters inhibit phorbol 12-myristate 13-acetate induced tumor promotion in CD-1 mouse skin. *Cancer Res* 1993;53:2507–12.

[5] Hennings H, Blumberg PM, Pettit GR, Herald CL, Shores R, Yuspa SH. Bryostatin 1, an activator of protein kinase C, inhibits tumor promotion by phorbol esters in SENCAR mouse skin. *Carcinogenesis* 1987;8:1343–6.

[6] Bocklandt S, Blumberg PM, Hamer DH. Activation of latent HIV-1 expression by the potent anti-tumor promoter 12-deoxyphorbol 13-phenylacetate. *Antiviral Res* 2003;59:89–98.

[7] Pettit GR. The bryostatins. *Fortschr Chem Org Naturst* 1991;57:153–95.

[8] Pasti G, Rivedal E, Yuspa SH, Herald CL, Pettit GR, Blumberg PM. Contrasting duration of inhibition of cell–cell communication in primary mouse epidermal cells by phorbol 12,13-dibutyrate and by bryostatin. *Cancer Res* 1988;48:447–51.

[9] Isakov N, Galron D, Mustelin T, Pettit GR, Altman A. Inhibition of phorbol ester-induced T cell proliferation by bryostatin is associated with rapid degradation of protein kinase C. *J Immunol* 1993;150:1195–204.

[10] Lee HW, Smith L, Pettit GR, Bingham Smith J. Dephosphorylation of activated protein kinase C contributes to downregulation by bryostatin. *Am J Physiol* 1996;271:C304–11.

[11] Szallasi Z, Denning MF, Smith CB, Dlugosz AA, Yuspa SH, Pettit GR, et al. Bryostatin 1 protects protein kinase C-delta from down-regulation in mouse keratinocytes in parallel with its inhibition of phorbol ester-induced differentiation. *Mol Pharmacol* 1994;46:840–50.

[12] Lorenzo PS, Bogi K, Acs P, Pettit GR, Blumberg PM. The catalytic domain of protein kinase Cdelta confers protection from down-regulation induced by bryostatin 1. *J Biol Chem* 1997;272:33338–43.

[13] Wang QJ, Bhattacharyya D, Garfield S, Nacro K, Marquez VE, Blumberg PM. Differential localization of protein kinase C delta by phorbol esters and related compounds using a fusion protein with green fluorescent protein. *J Biol Chem* 1999;274:37233–9.

[14] von Burstin VA, Xiao L, Kazanietz MG. Bryostatin 1 inhibits phorbol ester-induced apoptosis in prostate cancer cells by differentially modulating protein kinase C (PKC) (delta) translocation and preventing PKC(delta)-mediated release of tumor necrosis factor-(alpha). *Mol Pharmacol* 2010;78:325–32.

[15] Hale KJ, Manaviar S. New approaches to the total synthesis of the bryostatin antitumor macrolides. *Chem Asian J* 2010;5:4–54.

[16] Wender PA, Verma VA, Paxton TJ, Pillow TH. Function-oriented synthesis, scale economy, and drug design. *Acc Chem Res* 2008;41:40–9.

[17] Wender PA, DeBrabander J, Harran PG, Jimenez JM, Koehler MF, Lipka B, et al. The design, computer modeling, solution structure, and biological evaluation of synthetic analogs of bryostatin 1. *Proc Natl Acad Sci USA* 1998;95:6624–9.

[18] Keck GE, Kraft MB, Truong AP, Li W, Sanchez CC, Kedei N, et al. Convergent assembly of highly potent analogues of bryostatin 1 via pyran annulation: bryostatin look-alikes that mimic phorbol ester function. *J Am Chem Soc* 2008;130:6660–1.

[19] Powell CT, Britts NJ, Stec D, Hug H, Heston WD, Fair WR. Persistent membrane translocation of protein kinase C alpha during 12-O-tetradecanoylphorbol-13-acetate-induced apoptosis of LNCaP human prostate cancer cells. *Cell Growth Differ* 1996;7:419–28.

[20] Gschwend JE, Fair WR, Powell CT. Bryostatin 1 induces prolonged activation of extracellular regulated protein kinases in and apoptosis of LNCaP human

prostate cancer cells overexpressing protein kinase calpha. *Mol Pharmacol* 2000;57:1224–34.

[21] Gonzalez-Guerrico AM, Kazanietz MG. Phorbol ester-induced apoptosis in prostate cancer cells via autocrine activation of the extrinsic apoptotic cascade: a key role for protein kinase C delta. *J Biol Chem* 2005;280:38982–91.

[22] Yang D, Kedei N, Li L, Tao J, Velasquez JF, Michalowski AM, et al. RasGRP3 contributes to formation and maintenance of the prostate cancer phenotype. *Cancer Res* 2010;70:7905–17.

[23] Malolanarasimhan K, Kedei N, Sigano DM, Kelley JA, Lai CC, Lewin NE, et al. Conformationally constrained analogues of diacylglycerol (DAG). 27. Modulation of membrane translocation of protein kinase C (PKC) isozymes alpha and delta by diacylglycerol lactones (DAG-lactones) containing rigid-rod acyl groups. *J Med Chem* 2007;50:962–78.

[24] Wender PA, Verma VA. The design, synthesis, and evaluation of C7 diversified bryostatin analogs reveals a hot spot for PKC affinity. *Org Lett* 2008;10:3331–4.

[25] Hocevar BA, Morrow DM, Tykocinski ML, Fields AP. Protein kinase C isotypes in human erythroleukemia cell proliferation and differentiation. *J Cell Sci* 1992;101(Pt 3):671–9.

[26] Fujii T, Garcia-Bermejo ML, Bernabo JL, Caamano J, Ohba M, Kuroki T, et al. Involvement of protein kinase C delta (PKCdelta) in phorbol ester-induced apoptosis in LNCaP prostate cancer cells. Lack of proteolytic cleavage of PKCdelta. *J Biol Chem* 2000;275:7574–82.

[27] Garcia-Bermejo ML, Leskow FC, Fujii T, Wang Q, Blumberg PM, Ohba M, et al. Diacylglycerol (DAG)-lactones, a new class of protein kinase C (PKC) agonists, induce apoptosis in LNCaP prostate cancer cells by selective activation of PKCalpha. *J Biol Chem* 2002;277:645–55.

[28] Powell CT, Yin L. Overexpression of PKCepsilon sensitizes LNCaP human prostate cancer cells to induction of apoptosis by bryostatin 1. *Int J Cancer* 2006;118:1572–6.

[29] Rybin VO, Guo J, Steinberg SF. Protein kinase D1 autophosphorylation via distinct mechanisms at Ser744/Ser748 and Ser916. *J Biol Chem* 2009; 284:2332–43.

[30] Davies SP, Reddy H, Caivano M, Cohen P. Specificity and mechanism of action of some commonly used protein kinase inhibitors. *Biochem J* 2000;351:95–105.

[31] O'Neill RA, Bhamidipati A, Bi X, Deb-Basu D, Cahill L, Ferrante J, et al. Isoelectric focusing technology quantifies protein signaling in 25 cells. *Proc Natl Acad Sci USA* 2006;103:16153–8.

[32] Lamph WW, Wamsley P, Sassone-Corsi P, Verma IM. Induction of proto-oncogene JUN/AP-1 by serum and TPA. *Nature* 1988;334:629–31.

[33] Ikezoe T, Yang Y, Taguchi H, Koeffler HP. JNK interacting protein 1 (JIP-1) protects LNCaP prostate cancer cells from growth arrest and apoptosis mediated by 12-O-tetradecanoylphorbol-13-acetate (TPA). *Br J Cancer* 2004; 90:2017–24.

[34] Engedal N, Korkmaz CG, Saatcioglu F. C-Jun N-terminal kinase is required for phorbol ester- and thapsigargin-induced apoptosis in the androgen responsive prostate cancer cell line LNCaP. *Oncogene* 2002;21:1017–27.

[35] Durgan J, Michael N, Totty N, Parker PJ. Novel phosphorylation site markers of protein kinase C delta activation. *FEBS Lett* 2007;581:3377–81.

[36] Brodie C, Blumberg PM. Regulation of cell apoptosis by protein kinase C delta. *Apoptosis* 2003;8:19–27.

[37] Reyland ME. Protein kinase Cdelta and apoptosis. *Biochem Soc Trans* 2007;35:1001–4.

[38] Steinberg SF. Structural basis of protein kinase C isoform function. *Physiol Rev* 2008;88:1341–78.

[39] Gould CM, Newton AC. The life and death of protein kinase C. *Curr Drug Targets* 2008;9:614–25.

[40] Leontieva OV, Black JD. Identification of two distinct pathways of protein kinase Calpha down-regulation in intestinal epithelial cells. *J Biol Chem* 2004;279:5788–801.

[41] Gao T, Brognard J, Newton AC. The phosphatase PHLPP controls the cellular levels of protein kinase C. *J Biol Chem* 2008;283:6300–11.

[42] Parker PJ, Bosca L, Dekker L, Goode NT, Hajibagheri N, Hansra G. Protein kinase C (PKC)-induced PKC degradation: a model for down-regulation. *Biochem Soc Trans* 1995;23:153–5.

[43] Adams J. The development of proteasome inhibitors as anticancer drugs. *Cancer Cell* 2004;5:417–21.

[44] Cataisson C, Joeseloff E, Murillas R, Wang A, Atwell C, Torgerson S, et al. Activation of cutaneous protein kinase C alpha induces keratinocyte apoptosis and intraepidermal inflammation by independent signaling pathways. *J Immunol* 2003;171:2703–13.

[45] Keck GE, Li W, Kraft MB, Kedei N, Lewin NE, Blumberg PM. The bryostatin 1 A-ring acetate is not the critical determinant for antagonism of phorbol ester-induced biological responses. *Org Lett* 2009;11:2277–80.

[46] Keck GE, Poudel YB, Welch DS, Kraft MB, Truong AP, Stephens JC, et al. Substitution on the A-ring confers to bryopyran analogues the unique biological activity characteristic of bryostatins and distinct from that of the phorbol esters. *Org Lett* 2009;11:593–6.

[47] Keck GE, Poudel YB, Rudra A, Stephens JC, Kedei N, Lewin NE, et al. Molecular modeling, total synthesis, and biological evaluations of C9-deoxy bryostatin 1. *Angew Chem Int Ed Engl* 2010;49:4580–4.

[48] Tanaka Y, Gavrieliides MV, Mitsuchi Y, Fujii T, Kazanietz MG. Protein kinase C promotes apoptosis in LNCaP prostate cancer cells through activation of p38 MAPK and inhibition of the Akt survival pathway. *J Biol Chem* 2003; 278:33753–62.

837
838
839
840
841
842
843
844
845
846
847
848
849
850
851
852
853
854
855
856
857
858
859
860
861
862
863
864
865
866
867
868
869
870
871
872
873
874
875
876
877
878
879
880
881
882
883
884
885
886
887
888
889
890
891
892
893
894
895
896
897
898
899
900
901
902
903
904
905
906
907
908
909
910
911
912
913
914
915
916
917
918
919
920
921
922

- 923
924
925
926
927
928
929
930
931
932
933
934
- [49] Xiao L, Eto M, Kazanietz MG. ROCK mediates phorbol ester-induced apoptosis in prostate cancer cells via p21Cip1 up-regulation and JNK. *J Biol Chem* 2009;284:29365–7.
- [50] Xiao L, Gonzalez-Guerrico A, Kazanietz MG. PKC-mediated secretion of death factors in LNCaP prostate cancer cells is regulated by androgens. *Mol Carcinog* 2009;48:187–95.
- [51] Meshki J, Caino MC, von Burstin VA, Griner E, Kazanietz MG. Regulation of prostate cancer cell survival by protein kinase C{epsilon} involves bad phosphorylation and modulation of the TNF{alpha}/JNK pathway. *J Biol Chem* 2010;285:26033–40.
- [52] Truman JP, Rotenberg SA, Kang JH, Lerman G, Fuks Z, Kolesnick R, et al. PKCalpha activation downregulates ATM and radio-sensitizes androgen-sensitive human prostate cancer cells in vitro and in vivo. *Cancer Biol Ther* 2009;8:54–63.
- [53] Shih A, Zhang S, Cao HJ, Boswell S, Wu YH, Tang HY, et al. Inhibitory effect of epidermal growth factor on resveratrol-induced apoptosis in prostate cancer cells is mediated by protein kinase C-alpha. *Mol Cancer Ther* 2004;3:1355–64.
- [54] Blagosklonny MV, Dixon SC, Robey R, Figg WD. Resistance to growth inhibitory and apoptotic effects of phorbol ester and UCN-01 in aggressive cancer cell lines. *Int J Oncol* 2001;18:697–704.
- [55] Clamp A, Jayson GC. The clinical development of the bryostatins. *Anticancer Drugs* 2002;13:673–83.
- 935
936
937
938
939
940
941
942
943
944
945
- 946

UNCORRECTED PROOF